

4, at a width 7 kOe of the region of metastable states).

The nature of the magnetic inhomogeneities existing in the magnetic-field interval ΔH is most clearly illustrated by the correspondence of this interval (item 2 of Sec. 4) to the demagnetizing field of the sample $H_d = \beta \Delta M \approx 0.2$ kOe. Some excess of the observed value of ΔH can be understood by taking into account the inhomogeneity of the demagnetizing field in a sample of cubic shape, an inhomogeneity estimated in Sec. 4. According to the theory,¹² the demagnetizing field of the sample is the cause of the onset of an intermediate state in the sample during the first-order phase transition. It appears that in monoclinic NiWO_4 , just as in the uniaxial antiferromagnet MnF_2 ,¹¹ a domain structure is also realized in the magnetic-field interval ΔH , consisting of an alternation of regions of coexisting phases that are in statistical equilibrium with one another.

The authors are grateful to A. I. Zvyagin for supplying crystal NiWO_4 sample and for stimulating the undertaking of this research, and to V. V. Eremenko for support and discussion.

¹Hans von Weitzel, *Solid State Commun.* **8**, 2071 (1970).

²L. G. van Uitert, R. C. Sherwood, H. J. Williams, G. G. Rubin, and W. A. Bonner, *J. Phys. Chem. Solids* **25**, 1447 (1964).

³A. I. Zvyagin, A. G. Anders, A. I. Kut'ko, L. N. Pelikh, I. V. Skorobogatova, and V. G. Yurko, *Fizika nizkikh temperatur (Low Temperature Physics)*, No. XVIII, Khar'kov, 1972, p. 67.

⁴V. I. Kut'ko, V. M. Naumenko, and A. I. Zvyagin, *Fiz. Tverd. Tela (Leningrad)* **14**, 3436 (1972) [*Sov. Phys. Solid State* **14**, 2900 (1972)].

⁵V. V. Eremenko, Yu. G. Litvinenko, Yu. A. Popkov, T. I. Kazakova, and A. P. Mokhir, *Abstracts, 12th Internat. Conf. on Low-Temperature Physics and Technology, Szekesfehervar, Hungary, 1973.*

⁶Yu. G. Litvinenko, N. V. Gapon, and T. I. Kazakova, *Abstracts, 18th All-Union Conference on Low-Temperature Physics, Kiev, 1974.*

⁷E. A. Turov, *Fizicheskie svoystva magnitoporyadochennykh kristallov, (Physical Properties of Magnetically Ordered Crystals)*, Izd. Akad. Nauk SSSR, Moscow, 1963.

⁸M. I. Kaganov and G. K. Chepurnykh, *Fiz. Tverd. Tela (Leningrad)* **11**, 911 (1969) [*Sov. Phys. Solid State* **11**, 745 (1969)].

⁹V. A. Popov and V. I. Skidanenko, *Fizika kondensirovannogo sostoyaniya (Physics of the Condensed State)*, Physicotech. Inst. of Low Temp. Ukr. Acad. Sci., Vol. 7, Khar'kov, 1970.

¹⁰V. A. Popov and V. I. Skidanenko, *Ukr. Fiz. Zh.* **19**, 387 (1974).

¹¹K. L. Dudko, V. V. Eremenko, and V. M. Fridman, *Zh. Eksp. Teor. Fiz.* **61**, 678 (1971) [*Sov. Phys. JETP* **34**, 362 (1971)].

¹²V. G. Bar'yakhtar, A. E. Borovik, and V. A. Popov, *Pis'ma Zh. Eksp. Teor. Fiz.* **9**, 634 (1969) [*JETP Lett.* **9**, 391 (1969)].

Translated by J. G. Adashko

Spin-phonon interaction in a trigonal crystal

V. N. Vasyukov, S. N. Lukin, and G. A. Tsintsadze

*Cybernetics Institute, Georgian Academy of Sciences,
and Donetsk Physicotechnical Institute, Ukrainian Academy of Sciences*
(Submitted 20 April 1979)
Zh. Eksp. Teor. Fiz. **77**, 1544–1555 (October 1979)

The spin-phonon interaction (SPI) of Ni^{2+} ions in a trigonal zinc fluorosilicate ($\text{ZnSiF}_6 \cdot 6\text{H}_2\text{O}$) crystal is investigated. The complete set of the SPI tensor elements obtained from experiments on the effect of axial compression on the electron paramagnetic resonance (EPR) spectrum at 4.2 K is used to calculate the spin-lattice relaxation (SLR) time of the direct processes in the investigated system. A comparison of the calculated and experimental values shows good agreement when the phonon bottleneck effect is taken into account. The contribution of the crystal-lattice dynamics and of the temperature compressibility of the crystal to the initial splitting parameter D is calculated. It is established that the temperature compressibility and the SPI of the single-phonon processes do not describe the observed temperature dependence of D , while the SPI of two-phonon processes can describe this dependence.

PACS numbers: 63.20.Dj, 76.30.Fc

INTRODUCTION

The possibility of observing magnetic-resonance spectra and of practical utilization of diamagnetic crystals doped with paramagnetic ions in quantum-electronics devices is due greatly to the speed of the relaxation processes between the sublevels of the spin system. Numerous experimental and theoretical investigations have shown that when the paramagnetic

crystals are diluted the principal role can be assumed by the relaxation processes connected with energy transfer from the paramagnetic system to the phonon reservoir of the crystal lattice.

Theoretical calculations of the elements of the spin-phonon interaction (SPI) tensor¹ for cubic crystals lead to values that agree well with the experimental results. When the symmetry is lowered, however, the calcula-

tion of the SPI parameters becomes substantially more complicated, and the reliability of the obtained values is reduced. In the case of crystals with symmetry lower than cubic it becomes important therefore to determine experimentally the parameters of the phenomenological Hamiltonian.² The availability of these parameters permits a comparison of the calculated and experimental spin-lattice relaxation (SLR) times and leads to conclusions concerning the dominant mechanism of the relaxation process; this is important not only for the study of the magnetic-relaxation phenomenon, but also for the general laws of the kinetics as a whole.

On the other hand, the crystal-lattice dynamics, as shown in Refs. 3-5, influences via the SPI the parameters of the spin Hamiltonian that describes the electron paramagnetic resonance (EPR) spectrum, and is one of the mechanisms responsible for the temperature dependence of the observed spectra.

Among the experimental methods used to determine the SPI tensor elements, notice should be taken of two that yield the most reliable information, viz., acoustic electron paramagnetic resonances (AEPR) and the investigation of the influence of axial compression on the EPR spectra. The last method makes it possible to determine not only the value but also the sign of the SPI tensor elements and is technically simpler.

The SPI tensor elements have heretofore been determined in practice only for paramagnetic centers in crystals with cubic symmetry.^{6,7} The scarcity of experimental data on SPI in crystals of trigonal and tetragonal symmetry has not made it possible to determine the role of SPI in the EPR spectrum, in its temperature dependence, and in the corresponding relaxation processes.

The object of our study of SPI in noncubic crystals was chosen to be the model crystal zinc fluorosilicate ($ZnSiF_6 \cdot 6H_2O$) doped with divalent nickel ions, since both the SLR^{8,9} and the temperature dependence of the initial-splitting parameter^{10,11} were investigated in sufficient detail for this crystal.

FEATURES OF THE EXPERIMENTAL TECHNIQUE

The SPI tensor elements of the Ni^{2+} ion in the zinc fluorosilicate crystal were performed with a 4-mm band EPR spectrometer, using uniaxial compression of the investigated sample. All the measurements of the dependence of the EPR spectrum on the uniaxial compression were made at 4.2 K to exclude the possible temperature-dependent contribution to the dependence of the positions of the spectral lines on the pressure.

The high-grade zinc fluorosilicate crystals, grown by a previously described procedure,¹² contained 0.08% divalent nickel ions and about 0.01% divalent copper added for accurate orientation of the crystal. The nickel ion concentration was chosen to ensure reliable observation of the EPR signal, on the one hand, and to minimize the line width (and improve the accuracy) on the other.

The axial compression of the investigated sample was produced by a low-temperature bellows press with liquid helium as the working medium. Figure 1 shows a section through the uniaxial-compression unit, which occupied a small section of an "ultralong" resonator.¹³

The special measures taken in the apparatus (guides, ball 9, plane-parallel surfaces of the compression plate 2 and of the piston 4) and the painstaking preparation of the samples resulted in a highly homogeneous axial compression.

The investigated sample was a round cylinder with plane-parallel bases. The cylindrical surface was produced by boring out the sample at the required angle relative to the crystallographic axes of an optically homogeneous zinc-fluorosilicate crystal, using a hollow milling cutter with very sharp teeth. Using the lateral surface of the obtained cylinder as the basis, the end faces of the sample were lapped on a plane using diamond pastes with grain dimensions 5-1 μm .

The typical diameter of the used samples fluctuated in the interval 2.5-3.0 mm. At this diameter, and at a liquid-helium pressure in the bellows press 25 kg/cm², the uniaxial pressure reached 400-500 kg/cm². The crystal remained homogeneous and all the changes in the EPR spectrum were fully reversible.

CHOICE OF COORDINATE SYSTEM AND SINGULARITIES OF THE CRYSTAL STRUCTURE

To measure the elements of the SPI tensor it is necessary to choose a coordinate system. This system is usually referred to the outer faceting of the crystal, which constitutes for $ZnSiF_6 \cdot 6H_2O$ a combination of h hexagonal prism and a rhombohedron. The symmetry of this figure is described by the D_{3d} group. It is known from x-ray structure data¹⁴ that the symmetry of the crystal is described by the point group C_{3i} , which does not have the twofold axes and reflection planes present in D_{3d} .

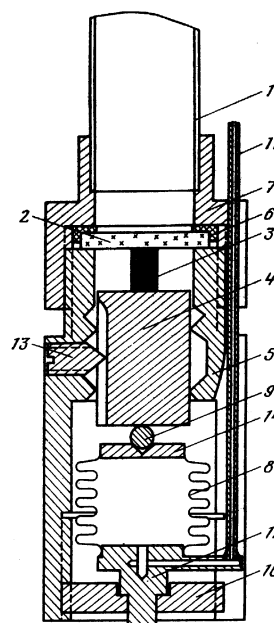


FIG. 1. Diagram of bellows press: 1—resonator, 2—quartz washer, 3—investigated sample, 4—piston, 5—body, 6—liner, 7—nut, 8—bellows, 9—ball, 10—movable base, 11—capillary, 12—lower plug, 13—guide screw, 14—upper plug.

The presence of additional elements in the symmetry group of the outer faceting leads to a possible ambiguous and nonequivalent choice of the coordinate system when the crystal is oriented relative to its habit. To eliminate the ambiguity it is necessary to orient the coordinate frame relative to the microscopic structure of the crystal. This was done here by using a low-temperature manifestation of the Jahn-Teller effect in the EPR spectrum of the Cu^{2+} ion in the $\text{ZnSiF}_6 \cdot 6\text{H}_2\text{O}$ crystal.¹⁵ To this end, a small admixture of Cu^{2+} ions was added to the crystals together with the Ni^{2+} impurity. The principal axes of the g -tensors of the low-temperature EPR spectrum of the Cu^{2+} ion in zinc fluorosilicate coincides with the fourfold axes of the H_2O -molecule octahedron. Measurement of the angular dependence of the EPR spectrum of the Cu^{2+} ion in the crystal makes it possible to determine the orientation of the principal axes of the g -tensor of the copper ion, and consequently also to tie in the coordinate system of the Ni^{2+} ion with the microscopic structure of the crystal. Figure 2 shows schematically the coordinate system used in the present study together with the external faceting of the crystal.

Special experiments aimed at determining the effect of axial pressure on the EPR spectrum in the orientations $[2^{-1/2}, 0, 2^{-1/2}]$ and $[2^{-1/2}, 0, -2^{-1/2}]$ revealed no differences, within the limits of the experimental errors, in the results, so that the D_{3d} group was used to describe the symmetry of the SPI tensor.

SPIN-PHONON INTERACTION HAMILTONIAN

The SPI of the paramagnetic ion in the crystal can be described phenomenologically with the aid of a Hamiltonian of the type

$$H_{\text{cph}} = \frac{1}{2} \sum_{\alpha\beta\gamma\delta} (S_\alpha S_\beta + S_\gamma S_\delta) G_{\alpha\beta\gamma\delta} e_{\gamma\delta}, \quad (1)$$

where S_α , $G_{\alpha\beta\gamma\delta}$, and $e_{\gamma\delta}$ are respectively the component of the spin operator, the element of the SPI tensor, and the element of the strain tensor. In the general case the SPI tensor has 36 independent elements. The assumption that the investigated crystal has D_{3d} symmetry decreases the number of independent elements to eight.

The condition $\text{Tr}H_{\text{cph}} = 0$ separates from the Hamiltonian (1) the part responsible for the splitting of the spin multiplet. For the D_{3d} symmetry, this condition

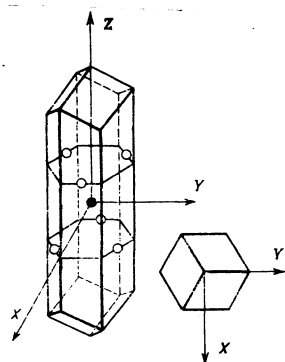


FIG. 2. Coordinate system together with the outer faceting of the $\text{ZnSiF}_6 \cdot 6\text{H}_2\text{O}$ crystal. The orientation of the nearest surrounding of the paramagnetic ion relative to the outer faceting is shown in arbitrary fashion. ●— Ni^{2+} , ○— H_2O .

reduces to the relations

$$G_{11} + G_{12} + G_{31} = 0, \quad 2G_{13} + G_{33} = 0. \quad (2)$$

We use in this paper the Voigt representation ($xx = 1, yy = 2, zz = 3, yz = 4, xy = 6$). The condition (2) reduces the number of independent parameters to six. The SPI matrix has for D_{3d} symmetry the form

$$\begin{pmatrix} G_{11} & G_{12} & G_{13} & G_{14} & 0 & 0 \\ G_{12} & G_{11} & G_{13} & -G_{14} & 0 & 0 \\ -G_{11} - G_{12} & -G_{11} - G_{12} & -1/2 G_{13} & 0 & 0 & 0 \\ G_{41} & -G_{41} & 0 & G_{44} & 0 & G_{41} \\ 0 & 0 & 0 & 0 & G_{44} & 0 \\ 0 & 0 & 0 & G_{14} & 0 & 1/2 (G_{11} - G_{12}) \end{pmatrix}. \quad (3)$$

If the magnetic-field and axial-pressure directions are specified relative to the chosen reference frame by the spherical coordinates θ and φ , then the Hamiltonian of the interaction of the spin of the investigated paramagnetic Ni^{2+} ion with the crystal strain produced by the external axial pressure P can be represented in the form

$$\begin{aligned} H_p = & -1/2 P (S_z^2 - 1/3 S(S+1)) \{ C_{33} \cos^2 \theta (3 \cos^2 \theta - 1) \\ & + C_{31} \sin^2 \theta (3 \cos^2 \theta - 1) - C_{13} \cos^2 \theta (3 \cos^2 \theta - 1) \\ & + C_{11} \sin^2 \theta [(3 \sin^2 \theta - 1) - 1/2 \sin^2 \theta \cos^2 \varphi \sin^2 \varphi] \\ & - C_{13} \sin^2 \theta [1 - 1/2 \sin^2 \theta \cos^2 \varphi \sin^2 \varphi] + 3C_{44} \cos^2 \theta \sin^2 \theta \\ & + 3(C_{41} + C_{14}) \cos \theta \sin^2 \theta \sin \varphi (3 \cos^2 \varphi - 1) \} + \text{O.T.} \end{aligned} \quad (4)$$

where the tensor C is defined as

$$C_{\alpha\beta\gamma\delta} = \sum_{mi} G_{\alpha\beta mi} S_{mi\gamma\delta}, \quad (5)$$

$S_{mi\gamma\delta}$ is an element of the crystal ductility tensor, and O.T. stands for the off-diagonal terms of the Hamiltonian.

The spin operators in (4) are given in a representation with the quantization axis along the magnetic field. The experimental conditions allow us to regard H_p as a perturbation compared with the Zeeman energy and to neglect the off-diagonal terms, which contribute to the energy of the spin states only in second order of perturbation theory in the ratio H_p/H_{Zeeman} .

It follows from (4) that when the pressure is directed along the magnetic field we can determine only five independent combinations of elements of the tensor C ; this is insufficient to obtain the six independent elements of the SPI tensor.

The Hamiltonian of the investigated SPI is the linear part, in the strain tensor, and the quadratic part, in the electron coordinates, of the energy of interaction of the paramagnetic ion with the crystal lattice. Calculations show that the SPI elements are proportional to the following expressions:

$$\begin{aligned} G_{11} = G_{44} & \sim \frac{45 \cos \alpha \sin^2 \alpha}{2R^2}, \\ G_{13} & \sim \frac{18 \cos^2 \beta}{r^4} (4 - 9 \sin^2 \beta) + \gamma \frac{18 \cos^2 \alpha}{R^2} (4 - 5 \sin^2 \alpha), \\ -G_{11} - G_{12} = G_{31} & \sim \frac{18 \sin^2 \beta}{r^4} (2 - 9 \cos^2 \beta) + \gamma \frac{9 \sin^2 \alpha}{R^2} (1 - 10 \cos^2 \alpha), \end{aligned} \quad (6)$$

where r and R are the respective distances from the paramagnetic ion to the ligand to the first (H_2O molecule) and second (the complex $[\text{SiF}_6]^{-2}$) coordination

spheres, β and α are the angles between the threefold axis of the crystal and the direction from the paramagnetic ion to the ligands of the first and second coordination spheres, and γ is a factor independent of r , R , α , or β .

Thus, $G_{14}=G_{41}$ for all values of α or β , while G_{13} and G_{31} are equal only if the complexes of the two nearest surroundings are regular figures, i. e., in the case of cubic symmetry of the crystal. These properties of the SPI tensor are not unique to the Ni^{2+} ion in the crystal $ZnSiF_6 \cdot 6H_2O$. The case of Cr^{3+} in Al_2O_3 is analogous.¹⁶

The aggregate of the properties of the elements of the tensor $G_{\alpha\beta\gamma\delta}$ makes it possible to describe the SPI in our case by five independent parameters, for the determination of which it suffices to investigate the influence of the axial pressure on the EPR spectrum for five compression directions.

MEASUREMENT RESULTS

We chose for the experiments the five axial-compression directions $[1, 0, 0]$, $[2^{-1/2}, 2^{-1/2}, 0]$, $[0, 0, 1]$, $[0, 2^{-1/2}, -2^{-1/2}]$, $[2^{-1/2}, 0, 2^{-1/2}]$.

When an axial pressure is applied to the crystal the EPR spectral lines change their positions in the magnetic fields and their widths in a fully reversible manner. The line shifts of the two allowed ($\Delta M_s = \pm 1$) transitions of the fine structure of the EPR spectrum of the Ni^{2+} ion are of equal magnitude and opposite sign. The center of gravity of this spectrum remains unchanged within the limits of the measurement accuracy. This is evidence that the Hamiltonian (1) greatly exceeds the SPI due to the modulation of the Zeeman term, and allows us to neglect the latter compared with (1).

To improve the reliability of the results, the experiment was performed on several samples for each direction. Figure 3 shows the dependence of the shift of the strong-field line of the EPR spectrum as obtained from the results of an experiment that is closest to the average.

As seen from the diagrams, the dependence of the EPR line positions on the pressure is well described by a linear function, thus justifying the use of an SPI Hamiltonian linear in the strain tensor. The coefficients of the linear dependences of the corresponding diagrams are listed together with their expressions in terms of the elements of the tensor C in Table I.

From the results of Table I, taking (5) into account, a system of fifth-order equations was formulated in terms of the elements of the SPI tensor. Solution of this equation leads to the values

$$\begin{aligned} G_{11} &= 23.2 \pm 4.9 \text{ cm}^{-1}, & G_{12} &= 24.1 \pm 4.9 \text{ cm}^{-1}, \\ G_{13} &= 2.3 \pm 2.2 \text{ cm}^{-1}, & G_{14} &= -0.14 \pm 0.72 \text{ cm}^{-1}, & G_{44} &= 13.5 \pm 1.6 \text{ cm}^{-1} \end{aligned} \quad (7)$$

To solve the system we used the values of the ductility tensor of the zinc fluorosilicate crystal, determined from the ultrasound propagation velocity at $T = 77$ K (Table II). Further lowering of the temperature 4.2 K leads to negligible changes, within the limits of the

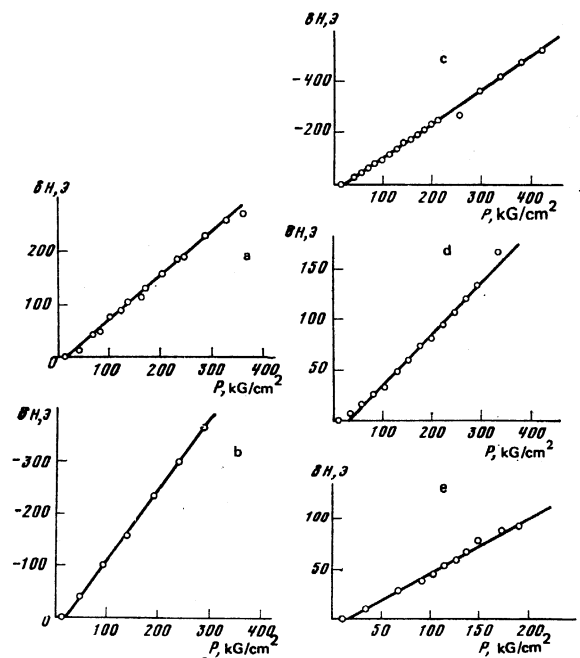


FIG. 3. Shift of strong-field line of EPR spectrum of Ni ion following axial compression applied in the directions: a— $[0, 0, 1]$, b— $[1, 0, 0]$, c— $[2^{-1/2}, 2^{-1/2}, 0]$, d— $[2^{-1/2}, 0, 2^{-1/2}]$, e— $[0, 2^{-1/2}, -2^{-1/2}]$.

measurement error, of the elastic properties of the crystal, and consequently we use throughout the results of ultrasound experiments at 77 K.

SPIN-LATTICE RELAXATION

It is known from the general SLR theory that the relaxation processes in a three-level system ($S=1$) are described by two relaxation times¹⁷:

$$(n_i - n_i^0) / (n_i^0 - n_j^0) = 1 + A_1 \exp(-t/T_1) + A_2 \exp(-t/T_2), \quad (8)$$

n_i and n_i^0 are the nonequilibrium populations of the level i ; T_1 and T_2 are the relaxation times; A_1 and A_2 are weighting factors.

The relaxation times and the weighting times expressed in terms of the probabilities of the relaxation processes can be represented in the form

$$\begin{aligned} T_{1,2}^{-1} &= w_{10} - w_{-10} + w_{1,-1} \pm \{ (w_{-10} - w_{1,-1})^2 + (w_{10} - w_{-10})(w_{10} - w_{-10}) \}^{1/2}, \\ A_1 &= \frac{3(w_{1,-1} + w_{10}) - 2T_1^{-1}}{2(T_1^{-1} - T_2^{-1})}, & |0\rangle \leftrightarrow | -1\rangle, \\ A_1 &= \frac{3(w_{1,-1} + w_{-10}) - 2T_1^{-1}}{2(T_1^{-1} - T_2^{-1})}, & |0\rangle \leftrightarrow |1\rangle, \\ A_2 &= -1 - A_1, \end{aligned} \quad (9)$$

w_{mn} is the probability of a transition, under the influence of the SPI, from the state m to the state n per unit time.

TABLE I.

Pressure direction	$\delta H/dP$, Oe \cdot kg $^{-1}$ \cdot cm 2
$[0, 0, 1]$	$3C_{33}/2g \beta = 0.881 \pm 0.018$
$[1, 0, 0]$	$-3C_{11}/2g \beta = -1.300 \pm 0.025$
$[2^{-1/2}, 2^{-1/2}, 0]$	$-3(5C_{11} + 3C_{12})/16g \beta = -1.33 \pm 0.025$
$[0, 2^{-1/2}, -2^{-1/2}]$	$3(C_{14} + C_{14} + C_{41} - C_{13} - C_{13})/8g \beta = 0.54 \pm 0.015$
$[2^{-1/2}, 0, 2^{-1/2}]$	$3(C_{44} - C_{13} - C_{13})/8g \beta = 0.51 \pm 0.015$

TABLE II.

$S, 10^{-4}$ (kg/cm ²) ⁻¹	$T=295\text{ K}$		$T=77\text{ K}$		$S, 10^{-4}$ (kg/cm ²) ⁻¹	$T=295\text{ K}$		$T=77\text{ K}$	
	S_{11}	S_{12}	S_{22}	S_{33}		S_{11}	S_{12}	S_{22}	S_{33}
	6.42±0.28	-2.60±0.28	2.57±0.08						

The following expressions for the transition probabilities were obtained in the Debye model for the D_{3d} symmetry:

$$w_{mn} = \frac{(E_m - E_n)^2 \exp((E_m - E_n)/kT)}{\exp((E_m - E_n)/kT) - 1} \Phi_{mn},$$

$$\Phi_{10} = \Phi_{-10} = \frac{1}{15\pi\rho\hbar^4} \left(\frac{2}{v_l^2} + \frac{3}{v_t^2} \right) (G_{11}^2 + G_{12}^2),$$

$$\Phi_{1,-1} = \frac{1}{15\pi\rho\hbar^4} \left(\frac{2}{v_l^2} + \frac{3}{v_t^2} \right) \{ (G_{11} - G_{12})^2 + 4G_{12}^2 \},$$
(10)

ρ is the density of the crystal, v_l and v_t are the velocities of sound with longitudinal and transverse polarization, and E_m is the energy of the m -th spin state.

Using the numerical values obtained above for the SPI parameters (7) at a temperature $T=2\text{ K}$ and at a microwave frequency $\nu=9.3\text{ GHz}$, we calculated the SLR rates T_1^{-1} and T_2^{-1} and the weighting factors A_1 and A_2 for both transitions of the fine structure of the EPR spectrum of the Ni^{2+} ion at an external magnetic-field orientation $H_0 \parallel z$. The results of the calculations together with the published data on the SLR rate in the investigated system are given in Table III.

We assumed in the calculation that the density of zinc fluorosilicate is $\rho=2.14\text{ g/cm}^3$, and the sound velocities in the longitudinal and transverse directions were obtained by averaging over the possible directions the experimentally observed values $v_l=3.63 \cdot 10^3$ and $v_t=1.83 \cdot 10^3\text{ m/sec}$.

It follows from Table III that the relaxation of the transition $|0\rangle \rightarrow |-1\rangle$ is described by the time T_1 , since the weighting factor A_2 in the term containing the time T_2 is small compared with A_1 . The relaxation of the transition $|0\rangle \rightarrow |1\rangle$ is described by the times T_1 and T_2 with coefficients that are close in value. When the population process is approximated by a single exponential the resultant value is T_{calc}^{-1} listed in Table III.

In the analysis of the results we must recognize that the SLR rates were determined in the experiment for real crystals with approximate paramagnetic-impurity density 0.1%. As noted in Ref. 8, at Ni^{2+} impurity-ion concentrations 0.1–0.7% the zinc fluorosilicate crystal exhibits a clearly pronounced phonon-bottleneck effect that can lengthen substantially the experimentally observed relaxation time. If the concentration dependence given in Ref. 8 for the SLR rate is extrapolated to a

TABLE III.

Relaxation transitions	T_1^{-1} , sec ⁻¹	T_2^{-1} , sec ⁻¹	A_1	A_2	T_{calc}^{-1} , sec ⁻¹	T_{exp}^{-1} , sec ⁻¹		
						$c=0.1\%$ [1]	$c=0.14\%$ [1]	$c=0.08\%$ [1]
$ 0\rangle \rightarrow 1\rangle$	16128	2835	-0.3732	-0.6288	4740	350	607	830
$ 0\rangle \leftrightarrow -1\rangle$	4097	68	-0.9999	-0.0001	4097	170	512	700

concentration of at least 0.02%, then for the transition $|0\rangle \rightarrow |-1\rangle T_{\text{exp}}^{-1} \approx 2 \cdot 10^3\text{ sec}^{-1}$, which coincides practically with the relaxation rate calculated from the elements of the SPI tensor.

It should be noted that calculation of the SLR rate on the basis of the SPI tensor, as presented above, yields a value closer to the experiment by one order of magnitude than the widely used calculation procedure described in Refs. 18 and 19. Thus, for the case of Ni^{2+} ions in zinc fluorosilicate, the calculated rate turns out to be $74\,000\text{ sec}^{-1}$, and this rate and a similar degree of agreement between calculation and experiment are usually regarded as reasonable in the few papers where similar comparisons are made for impurity ions of the iron group (e.g., Ref. 20).

TEMPERATURE DEPENDENCE OF INITIAL SPLITTING

A number of EPR studies have revealed a temperature dependence of the initial splitting of the spin multiplet of the ground state of the paramagnetic ion. The observed dependence is frequently attributed to the temperature-induced compressibility of the crystal, due to the anharmonicity of the crystal-lattice vibrations via the SPI can also exert a substantial influence on the character of this temperature dependence.

The system $\text{ZnSiF}_6 \cdot 6\text{H}_2\text{O}$ with Ni^{2+} impurity, which is investigated here, demonstrates the strong temperature dependence of the axial initial splitting parameter D .^{10,11} The contribution of the temperature compressibility of this crystal to this dependence can be calculated on the basis of the results of a study of the connection between the parameter D and the features of the geometry of the nearest surroundings of the paramagnetic ion. The approach developed in Ref. 21 makes it possible to calculate the change of the parameter $D=D_0 + \delta D_{tc}$ with changing temperature on account of the change of the form of the paramagnetic complex:

$$\delta D_{tc} = \frac{\partial D}{\partial \beta} \frac{2^{\frac{1}{2}}}{3} \int_0^{\pi} (\sigma_{\perp} - \sigma_{\parallel}) dT, \quad (11)$$

where $\sigma_{\parallel}, \sigma_{\perp}$ are the coefficients of the longitudinal and transverse temperature compressibility of the crystal, T is the temperature, $\partial D/\partial \beta$ is a temperature-independent parameter equal to $-57.5\text{ cm}^{-1}/\text{rad}$ for the Ni^{2+} ion, and D_0 is the initial splitting parameter at the temperature 0 K.

A plot^{10,11} of $D(T)$ shows that at temperatures above the Debye temperature (T_D) the plot is nearly linear, and to compare the contributions of various mechanisms to the temperature dependence of the initial splitting it is convenient to consider the derivative taken at room temperature.

For the mechanism connected with the temperature expansion of the crystal we get from (11)

$$\frac{dD}{dT} = \frac{\partial D}{\partial \beta} \frac{2^{\frac{1}{2}}}{3} (\sigma_{\perp} - \sigma_{\parallel}). \quad (12)$$

In the considered case of the Ni^{2+} ion

$$(dD/dT)_{T=295\text{K}}^{\text{calc}} = 16.0 \cdot 10^{-4}\text{ cm}^{-1}\text{ deg}^{-1}.$$

To calculate the derivative we used the data of Ref. 22 on the temperature expansion of nickel fluorosilicate crystals, obtained in the temperature interval 0–25 °C:

$$\sigma_{\parallel} = 0.50 \cdot 10^{-1} \text{ deg}^{-1}, \quad \sigma_{\perp} = -0.095 \cdot 10^{-1} \text{ deg}^{-1}.$$

The experimentally observed¹¹ value

$$(\delta D/dT)_{T=295\text{K}}^{\text{exp}} = -15.2 \cdot 10^{-4} \text{ cm}^{-1} \text{ deg}^{-1}$$

is of opposite sign and of the same order of magnitude. Thus, the temperature compressibility of the crystal does not account for the observed variation of the initial-splitting parameter.

To calculate the contribution made to the parameter D by the SPI with the Hamiltonian (1), we used the results of Refs. 23 and 24, according to which the imaginary part of the susceptibility, which describes the absorption of the electromagnetic-radiation energy in EPR, is proportional to

$$\chi'' \propto \sum_{mn} \frac{\text{Re } \Gamma_{mn}}{(\omega - \omega_{mn} - \text{Im } \Gamma_{mn})^2 + (\text{Re } \Gamma_{mn})^2}, \quad (13)$$

where ω is the cyclic frequency of the microwave field, $\omega_{mn} = (E_m - E_n)/\hbar$, E_m and E_n are the energies of the corresponding spin states, and Γ_{mn} can be calculated by following Ref. 24.

Calculations of the dependence of the initial-splitting parameter on the features of the crystal-lattice dynamics for the case of paramagnetic ion with spin $S = 1$ in a field of trigonal symmetry lead to separation of two terms. The first is the temperature-independent contribution of the so-called zero-point oscillations

$$\delta D_0^{(1)} = \frac{\omega_{\text{Deb}}^3}{120\pi^2 \rho v_i^3} \{ (G_{11} + G_{12} - 2G_{13})^2 - 2(G_{11} - G_{12})^2 + 4G_{11}^2 - 4G_{12}^2 \}, \quad (14)$$

(ω_{Deb} , ρ , and v_i are respectively the Debye frequency, the crystal density, and the speed of sound with transverse polarization). The second term is the temperature-dependent contribution.

The numerical value of $\delta D_0^{(1)}$ calculated from the known elements of the SPI tensor is equal to 0.008 cm^{-1} . In the calculation of $\delta D_0^{(1)}$ we used the value $\omega_{\text{Deb}} = 1.28 \cdot 10^{13} \text{ sec}^{-1}$, calculated from the elastic properties of the crystal at 77 K.

The temperature-dependent phonon contribution is proportional to the temperature at high temperatures. The derivative dD/dt is calculated from the expression

$$\left(\frac{dD}{dT} \right)_{T=295\text{K}} = \frac{k \omega_{\text{Deb}} \delta D_0^{(1)}}{60\pi^2 \rho v_i^3 \hbar^2} (G_{11} + G_{12} - 2G_{13})^2, \quad (15)$$

where k is Boltzmann's constant.

The numerical value

$$(\delta D/dT)_{T=295\text{K}} = -10^{-7} \text{ cm}^{-1} \text{ K}^{-1}$$

obtained for our case has the same sign as the experimentally obtained temperature dependence, but its magnitude differs by four decades.

In addition to the considered mechanism, which is linear in the strain tensor, another contribution to the

initial splitting is made by the coupling of the magnetic spin with the phonon reservoir via an interaction quadratic in the strain tensor (two-phonon processes). The contribution of this last interaction to the parameter D is of the form²⁵

$$\delta D^{(2)} = K_D \left(\frac{T_{\text{Deb}}^4}{8} + T^4 \int_0^{T_{\text{Deb}}/T} \frac{x^3 dx}{e^x - 1} \right), \quad (16)$$

where K_D is expressed in terms of the SPI tensor elements of the two phonon processes $R_{\alpha\beta\gamma\delta\mu}$ in the following manner:

$$K_D = \frac{k^2}{30\pi^2 \rho v_i^3 \hbar^2} \left\{ 2 \sum_{\Gamma} (R_{\Gamma\Gamma\Gamma\Gamma\Gamma} - R_{\Gamma\Gamma\Gamma\Gamma}) + \sum_{\Gamma=0} (R_{\Gamma\Gamma\Gamma\Gamma\Gamma} - R_{\Gamma\Gamma\Gamma\Gamma}) - \sum_{\Gamma=0} (R_{\Gamma\Gamma\Gamma\Gamma\Gamma} - R_{\Gamma\Gamma\Gamma\Gamma}) \right\}. \quad (17)$$

The first term of (16) describes the temperature-independent contribution of the zero-point oscillations, and the second describes the sought temperature dependence of the parameter D .

We did not determine here the tensor elements R because they are relatively small and because of experimental difficulties. It is possible, however, to estimate these elements from the possible deviation of the shifts of the resonance transitions of the EPR spectrum from linearity upon application of axial pressure, and from the observed temperature dependence of D .

The maximum possible deviation of $H(P)$ from linearity (see Fig. 3), which does not exceed the experimental error, yields for the tensor elements an upper bound $R \leq 10^3 \text{ cm}^{-1}$.

The value of K_D determined from the experimentally observed¹¹ temperature dependence of D and from $T_{\text{Deb}} = 97.5 \text{ K}$ is equal to $K_D = 5 \cdot 10^{-9} \text{ cm}^{-1} \text{ K}^{-1}$. Knowing K_D , we can obtain from (17) a lower bound of the tensor elements: $R > 0.1 \text{ cm}^{-1}$.

Considering the temperature dependence of the initial splitting as a whole, it should be noted that the temperature expansion of the crystal does not influence significantly the deformation of the observed quantity D . When this mechanism is taken into account, the estimates given above for the tensor elements R must be corrected. The resultant interval of possible values ($0.2 \text{ cm}^{-1} < R < 10^3 \text{ cm}^{-1}$) indicates that the SPI of the Ni^{2+} ions via two-phonon processes, together with the temperature compressibility of the considered crystal, can account for the observed temperature dependence of the initial-splitting parameter:

¹R. D. Mattuek and M. W. P. Strandberg, Phys. Rev. **119**, 1204 (1960).

²N. G. Koloskova, In: Paramagnitnyĭ rezonans (Paramagnetic Resonance), No. 2, Kazan' Univ. Press, 1964, p. 115.

³L. K. Aminov and B. I. Kochelaev, Fiz. Tverd. Tela (Leningrad) **4**, 1604 (1962) [Sov. Phys. Solid State **4**, 1175 (1962)].

⁴V. A. Timofeev, Fiz. Tverd. Tela (Leningrad) **11**, 2353 (1969) [Sov. Phys. Solid State **11**, 1897 (1969)].

⁵V. A. Timofeev, Kristallografiya **15**, 742 (1970) [Sov. Phys. Crystallogr. **15**, 638 (1971)].

⁶E. B. Tucker, Proc. IEEE **53**, 1547 (1965).

- ⁷V. A. Golenishchev-Kutuzov, V. V. Samartsev, N. K. Solovarov, and B. M. Khabibulin, *Magnitnaya kvantovaya akustika (Magnetic Quantum Acoustics)*, Nauka, 1977.
- ⁸R. M. Valishev, Candidate's dissertation, Kazan' State Univ., 1966.
- ⁹V. N. Vasyukov, G. N. Neĭlo, A. D. Prokhorov, and G. A. Tsintsadze, *Fiz. Tverd. Tela (Leningrad)* **19**, 2389 (1977) [*Sov. Phys. Solid State* **19**, 1399 (1977)].
- ¹⁰S. N. Lukin, Candidate's Dissertation, Donetsk Physicotech Inst., 1975.
- ¹¹R. S. Rubins and S. K. Jani, *J. Chem. Phys.* **66**, 3297 (1977).
- ¹²N. G. Kabanova, S. N. Lukin, G. N. Neĭlo, and L. F. Chernysh, *Kristallografiya* **21**, 1235 (1976) [*Sov. Phys. Crystallogr.* **21**, 716 (1976)].
- ¹³S. N. Lukin, E. D. Nemchenko, and L. G. Oranskii, *Prib. Tekh. Eksp. No. 4*, 116 (1974).
- ¹⁴R. W. G. Wyckoff, *Crystal Structures*, 3, Interscience, 1951.
- ¹⁵B. Bleaney and K. D. Bowers, *Proc. Phys. Soc. London* **A65**, 667 (1952).
- ¹⁶R. B. Hemphill, P. L. Donoho, and E. D. McDonald, *Phys. Rev.* **146**, 329 (1966).
- ¹⁷N. B. Karlov and A. A. Manenkov, *Itogi nauki, Radiofizika. Kvantovye usiliteli (Science Summaries, Radiophysics, Quantum Amplifiers)* VINITI, 1966, p. 62.
- ¹⁸R. Orbach, *Proc. Phys. Soc. London* **A264**, 458 (1961).
- ¹⁹K. W. H. Stevens, *Rep. Prog. Phys.* **30**, 189 (1967).
- ²⁰K. P. Lee and D. Walsh, *Can. J. Phys.* **47**, 1753 (1969).
- ²¹V. N. Vasyukov, S. N. Lukin, and G. A. Tsintsadze, *Fiz. Tverd. Tela (Leningrad)* **20**, 2260 (1978) [*Sov. Phys. Solid State* **20**, 1304 (1978)].
- ²²W. M. Walsh, *Phys. Rev.* **114**, 1473 (1959).
- ²³L. K. Aminov, *Zh. Eksp. Teor. Fiz.* **48**, 1398 (1965) [*Sov. Phys. JETP* **21**, 934 (1965)].
- ²⁴L. K. Aminov, In: *Paramagnitnyĭ rezonans (Paramagnetic Resonance)*, No. 3, Kazan' Univ. Press, 1968, p. 3.
- ²⁵N. Shrivastava, *Phys. Rep.* **C20**, 137 (1975).

Translated by J. G. Adashko

Crystal optics of phases with incommensurable superstructures

V. A. Golovko and A. P. Levanyuk

Moscow Evening Metallurgical Institute

(Submitted 25 April 1979)

Zh. Eksp. Teor. Fiz. **77**, 1556-1574 (October 1979)

The characteristics of linear and nonlinear crystal optics in dielectrics with incommensurable superstructures are investigated theoretically for the case of ammonium fluoroberyllate. The optical properties can be described by a spatially periodic distribution of the dielectric constant and nonlinear susceptibility tensors which depend on the order parameter. The form of the tensors can be established on the basis of the phenomenological theory. The fields are determined by solving the Maxwell equations. Effects similar to the spatial dispersion effects, but more pronounced, are found. Moreover, a periodic dependence of the reflection coefficient on the position of the boundary with respect to the superstructure, and the appearance of ellipticity in the reflected light, are predicted. For the nonlinear properties it is shown that there is noticeable second harmonic generation due to low local symmetry. The influence of the surface results in the appearance of additional components of the harmonic field and in their periodic dependence on the position of the boundary with respect to the superstructure. This is most manifest on propagation of the wave along the axis of the superstructure. Qualitative agreement is observed between the theory and the only known experiment on second harmonic generation by the incommensurable phase. Quantitatively, however, the difference is appreciable and may be ascribed to the domain structure of the incommensurable phase. The analysis shows that the existence of a multidomain structure may result in a considerable increase of harmonic generation in the incommensurable phase.

PACS numbers: 78.20.Dj, 78.20.Bh, 42.65.Cq

Phases with incommensurable superstructures whose periods greatly exceed the interatomic distances but are smaller than the optical wavelengths λ have by now been observed in a large number of dielectrics (see, e.g., Refs. 1-3). It is natural to expect the propagation of light in such structures to have certain singularities, particularly those similar to the singularities known from crystal optics with spatial dispersion. The presence of spatial dispersion leads to a number of qualitatively new effects, the magnitude of which is determined by the ratio a/λ or $(a/\lambda)^2$, where a is the

radius of the intermolecular interaction.⁴ On the other hand, optical effects due to the superstructure should be determined by an analogous parameter in which a is replaced by d , where d is the period of the superstructure, and must therefore be much more strongly pronounced and much easier to observe in experiment.

One can hope that an experimental study of the optical properties of incommensurable phases will yield new data on their structure and singularities. The results of the first experiments⁵ turned out to be quite inter-